

# EVALUATION OF SATELLITE AERODYNAMIC AND RADIATION PRESSURE ACCELERATION MODELS USING ACCELEROMETER DATA

*Eelco Doornbos*

Delft University of Technology, Faculty of Aerospace Engineering

## ABSTRACT

Models of non-gravitational accelerations, of which satellite aerodynamics and radiation pressure are the most important examples, are critical for many orbit determination and prediction applications. Such models typically consist of three parts, each of which can be implemented at various levels of sophistication, depending on the required accuracy of the application. The first part consists of a model of the environment, such as the density of the atmospheric particles, or the direction and magnitude of the photon flux coming from the Sun and Earth. The second part is a model of the geometry and material properties of the satellite's outer surfaces, while the third part is a representation of the interaction between the particles and the surfaces. In its most simple form, these last two parts combined can be expressed in terms of a constant satellite ballistic coefficient.

Traditionally, the implementation of non-gravitational models in astrodynamics tools is based on a semi-empirical approach, and their assessment is based on an evaluation of tracking data residuals. The accelerometers on the CHAMP, GRACE, GOCE and Swarm satellites, however, measure the sum of the non-gravitational accelerations directly. The combination of these observations with non-gravitational acceleration models has led to the availability of thermospheric data sets with many scientific applications in the field of aeronomy.

In this paper, the experience obtained with the processing of accelerometer data and the use of non-gravitational force models for aeronomy applications is demonstrated, and applied in order to provide useful pointers for the implementation of such models in orbit determination and prediction tools at various levels of complexity and accuracy.

## 1. INTRODUCTION

The foundation of the field of astrodynamics is the application of the law of gravitational attraction to the motion of objects in space. However, non-gravitational accelerations can be equally important due to the high area to mass ratios and low altitudes of spacecraft. The two most important types are the aerodynamic and radiation pressure accelerations. The detail of implementation of models of these accelerations depends heavily on the application, and its required accuracy.

For example, for orbital lifetime calculations for low Earth orbiting satellites, the drag acceleration is obviously the driving force. Radiation pressure accelerations can be neglected, except in rare cases where radiation pressure can induce significant changes to the perigee altitude of highly elliptical orbits.

Non-gravitational forces, or surface forces as they are also sometimes called, require models consisting of three parts. The first part is a model of the environment, such as the density of the atmospheric particles, or the direction and magnitude of the photon flux coming from the Sun and Earth. The second part is a model of the geometry and material properties of the satellite's outer surfaces. The third part is a representation of the interaction between the particles and the surfaces, for example in terms of energy and momentum exchange.

Traditionally, the most accurate force models had to be applied in the precise orbit determination for satellites carrying radar altimeters for measuring sea surface height, or satellites carrying synthetic aperture radars (SAR) for SAR interferometry applications. The assessment of non-gravitational force model implementations for these applications was based on an evaluation of tracking data residuals that are obtained during an orbit determination process (1), based, for example, on satellite laser ranging, DORIS and/or GPS tracking data. The better the force models, the lower the tracking data residuals. However, there are many other factors that can affect these residuals, such as tracking data quality, measurement model uncertainty and gravity field model errors. The common use of empirical accelerations and other force model parameters that can cover up model weaknesses, regardless of their origin, in a reduced-dynamic orbit determination approach, makes the evaluation of non-gravitational force model quality even more difficult.

The accelerometers on the CHAMP (2), GRACE (3), GOCE (4) and Swarm satellites (5), however, measure the sum of the non-gravitational accelerations directly. The availability of these observations, processed in combination with state-of-the-art non-gravitational acceleration models, has led to the availability of thermospheric data sets with numerous scientific applications (6).

In this paper, the experience obtained with the processing of accelerometer data and the use of non-gravitational force models for aeronomy applications is demonstrated. This ex-

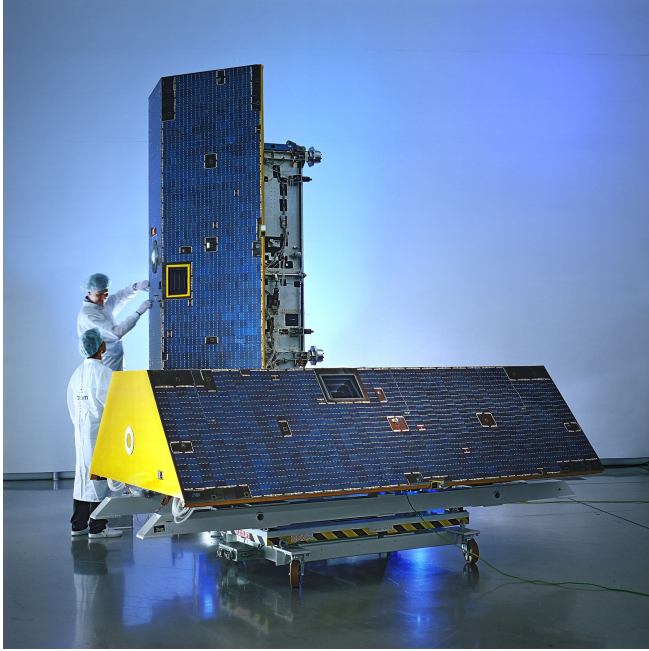


**Fig. 1.** The GRACE satellites. Photo courtesy of Astrium GmbH.

perience is used in order to provide useful pointers for the implementation of all three parts of non-gravitational force models in orbit determination and prediction tools at various levels of complexity and accuracy.

## 2. NON-GRAVIATIONAL ACCELERATION MEASUREMENTS

The launch of the German CHAMP satellite mission on July 17, 2000, signaled the start of an era of continuous high-resolution measurements of non-gravitational accelerations in space. Compared to earlier satellites that carried an accelerometer, CHAMP benefitted from its near-circular polar orbit, allowing the delivery of near-continuous global measurements, as well as the presence of precise star cameras for attitude determination and a high-end GPS receiver for orbit determination and calibration of the low-frequency content of the accelerometer data.

The twin GRACE satellites, launched in March 2002, the GOCE mission, launched in March 2009, and the three Swarm satellites, launched in November 2013 have ensured continuation of this data set, as well as delivered an increased spatial sampling during the mission overlap periods.

This paper will make use of the acceleration measurements made by CHAMP and GRACE, calibrated and further processed at Delft University of Technology, as well as models of these accelerations used in the thermosphere data processing. The references (7; 6) give further information on the calibration, data processing procedures and models used. An

Model	CHAMP		GRACE-A	
	$\mu^*$	$\sigma^*$	$\mu^*$	$\sigma^*$
Jacchia 71	0.670	1.274	0.726	1.407
DTM-78	0.688	1.348	0.678	1.569
MSIS-86	0.706	1.284	0.744	1.406
DTM-94	0.705	1.358	0.724	1.556
NRLMSISE-00	0.710	1.274	0.753	1.394
Jacchia-Bowman 2006	0.731	1.248	0.831	1.388
Jacchia-Bowman 2008	0.789	1.237	0.910	1.377
HASDM	0.813	1.163	0.984	1.284

**Table 1.** Log-normal statistics of accelerometer-derived over model density ratios for CHAMP and GRACE, comparing various models.

error estimate of the resulting density and crosswind data is included in these references as well.

## 3. AERODYNAMIC ACCELERATION MODELLING

### 3.1. Thermosphere density

The most important model of the space environment used in orbit prediction and orbit propagation of low Earth orbiting satellites is without a doubt the model of thermospheric density, applied in drag acceleration computations. The space science community has built up a considerable level of understanding of the behaviour of the thermosphere, through the use of physical first-principle models of the coupled ionosphere-thermosphere system, with some models also including coupling effects with models of the magnetosphere or lower layers of the atmosphere. The computational requirements of these models prohibit their use in orbit calculations.

Therefore, in most astrodynamics applications, empirical thermosphere models are used instead. The Jacchia (8; 9), MSIS (10) and DTM (11) model families are the most widely known and often used.

Table 1 provides a quality assessment of various empirical thermosphere models, made using the CHAMP and GRACE data during the years 2002-2007. The values in the table are based on densities obtained from the accelerometer data. For each data point, the density observation is divided by the corresponding model density. Such density ratios tend to have a log-normal distribution, and therefore the log-normal mean  $\mu^*$  and log-normal standard deviation  $\sigma^*$  are used to assess the quality of the models, which is better when the values are closer to one. The mean ( $\mu^*$ ) values represent scale differences, and these are in general caused by errors in both the density models and data, related to uncertainties in drag coefficients and the geometry of the satellites, as explained in more detail in (6). The  $\sigma^*$  values are a more valuable quality indicator. It is clear that for the period under consideration, the Jacchia-Bowman 2008 model performs best in this regard.

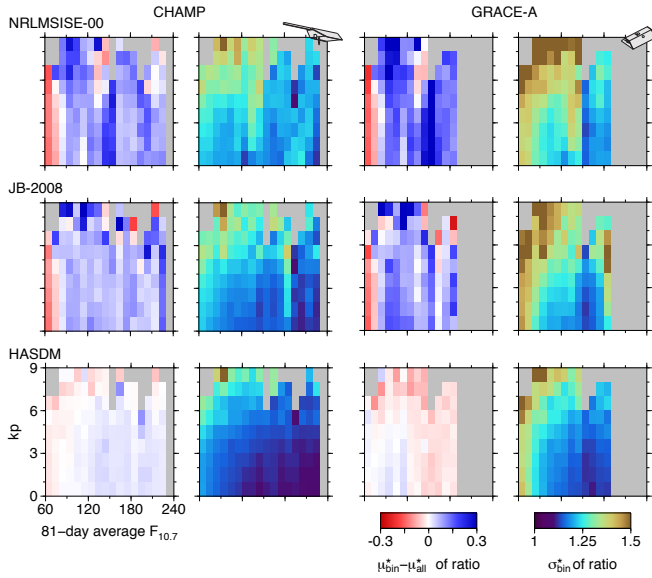


**Fig. 2.** Log-normal mean and standard deviations, binned by level of solar and geomagnetic activity, of CHAMP and GRACE-A data/model density ratios, for three different models.

However, different results have been obtained for other time periods, and especially for higher altitudes than CHAMP and GRACE. So the question of which density model should be recommended for which applications remains a difficult one to answer.

The list in Table 1 also includes the results of the HASDM model (12), which is a version of the Jacchia model that is automatically calibrated by making use of data on the orbital decay of many objects tracked by the US Space Surveillance Network. The HASDM data, evaluated along the CHAMP and GRACE tracks was kindly provided by Bruce Bowman. It is clear that this density model calibration approach results is succesful. Unfortunately, the model is not generally available, and so it cannot be readily applied in the orbit determination of other missions.

Figure 2 gives another view at the same data. In this case, the many millions of data/model density ratios that were summarized in the Table above have been binned with respect to the level of solar and geomagnetic activity, represented by the levels of the 81-day average of  $F_{10.7}$  (X-axis) and the planetary geomagnetic index  $k_p$  (Y-axis), respectively. The plots for the means, with the red-blue colour scale, indicates that there are considerable differences in model biases between low and high solar activity. All three models severely overestimate the density at low solar activity.

The standard deviations in these plots, on the other hand, are lowest for the combination high solar activity and low geomagnetic activity. This can be explained by the fact that the atmosphere shows large amplitude fluctuations in density at high solar activity, which is difficult for the models to repre-

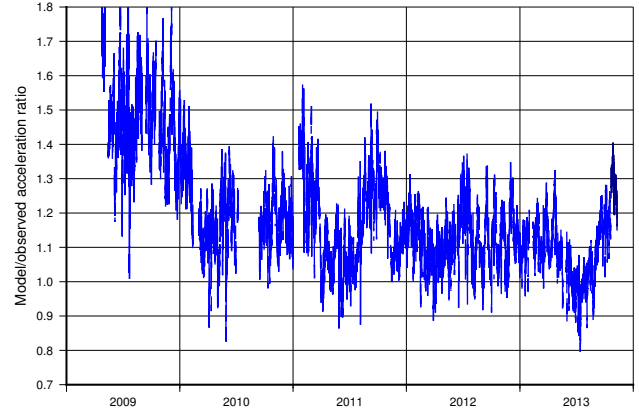


**Fig. 3.** Per-orbit ratio of NRLMSISE-00 density over GOCE accelerometer-derived density, for the entire mission duration.

sent. At high geomagnetic activity on the other hand, there is a good density/acceleration signal, which leads to improved accelerometer data processing results.

### 3.2. Pitfall of drag coefficient or ballistic coefficient estimation

In many practical cases, it is not possible to built a detailed aerodynamic model of a satellite or piece of space debris, simply because information on the geometry, attitude and/or mass are not available. In addition, it is known that empirical models might have biases, and are subject to long-term changes. Under such circumstances, it is customary to make an estimate of the ballistic coefficient, or the drag coefficient in an orbit estimation run using an empirical atmosphere model, over some duration, and apply this estimate in subsequent orbit propagation and orbit determination runs.

It is important to realise that such an estimate of, let's say, a ballistic coefficient, does not only contain information on the physical ballistic coefficient, but also on the error in the density model during the tracking time span of the orbit estimation run. Figure 3 shows an assessment of this error for the duration of the GOCE satellite, which was launched in March 2009, at the end of the last deep solar minimum. The Figure shows the ratios for the orbit-averaged NRLMSISE-00 density over the orbit-averaged acceleration-derived density. For a large part of 2009, the NRLMSISE-00 density was more than 1.4 times larger than the observed density. As solar activity decreased, so did the offset in the mean density, but during the entire mission, there were large fluctuations at the time scale of the solar rotation period (approximately 27 days). This plot therefore illustrates the danger in applying a ballistic coefficient estimate made at one point in time, to orbit prediction, or to orbit determination in other points in time.

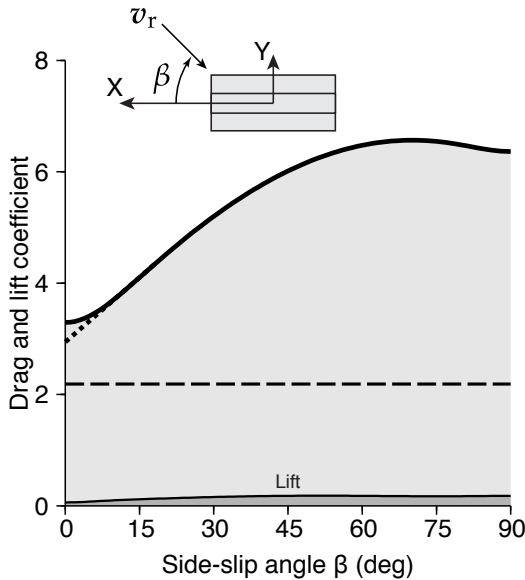


**Fig. 4.** Variation of the drag and lift coefficient, as modelled for the GRACE satellite.

### 3.3. Thermosphere wind

The modelling of the relative velocity of the atmospheric particles with respect to the satellite surfaces is another aspect for consideration. By far the largest term is the inertial orbital velocity, of about 7.5 km/s for low circular Earth orbits. The corotation of the atmosphere, and winds with respect to this corotating atmosphere are both of the order of 0.5 km/s. Wind effects tend to cancel when integrated over an orbit revolution. Wind models, like HWM (13), are therefore only used only in applications requiring the highest possible accuracy.

### 3.4. Limitations of the hyperthermal flow assumption

Figure 4 shows an example of how the influence of the level of sophistication of satellite aerodynamic models can affect the accuracy of the density data derived from the accelerations. The solid line represents the most accurate particle-surface interaction model, combined with a detailed geometry model. This model takes into account the momentum exchange due to the thermal motion of the gas particles, which is a function of the temperature and composition of the atmospheric gas. The dotted line shows what the slope of the curve would look like for low side-slip angles, in case of a hyperthermal approximation, using the same realistic satellite geometry model. In this case, the satellite's surface panels that are (nearly) parallel to the flow do not contribute (significantly) to the drag, causing a sharp decrease in drag for low sideslip angles. Koppenwallner (14) and Sutton (15) showed that this sharp decrease is unrealistic.

The dashed line, on the other hand, shows the most simple model imaginable, a "cannonball" with a constant frontal

area and drag coefficient. It is important to note here that when the sideslip angle remains small, as is the case under the nominal attitude control for satellites such as GRACE, the cannonball model actually provides a more accurate representation of the variation of the drag force with the side-slip angle than a model with a sophisticated geometry representation, but based on a hyperthermal flow assumption.

A "cannonball", or fixed ballistic coefficient model is used very often in astrodynamics applications, and turns out to be a very good approximation, for compact objects, for elongated objects with a fixed orientation with respect to the flow, and for rapidly tumbling objects. A more sophisticated model will be necessary for the most precise applications, and in the case of elongated or otherwise irregularly shaped objects, which are either slowly tumbling, or attitude-controlled in a way that causes large fluctuations in frontal area.

## 4. RADIATION PRESSURE MODELLING

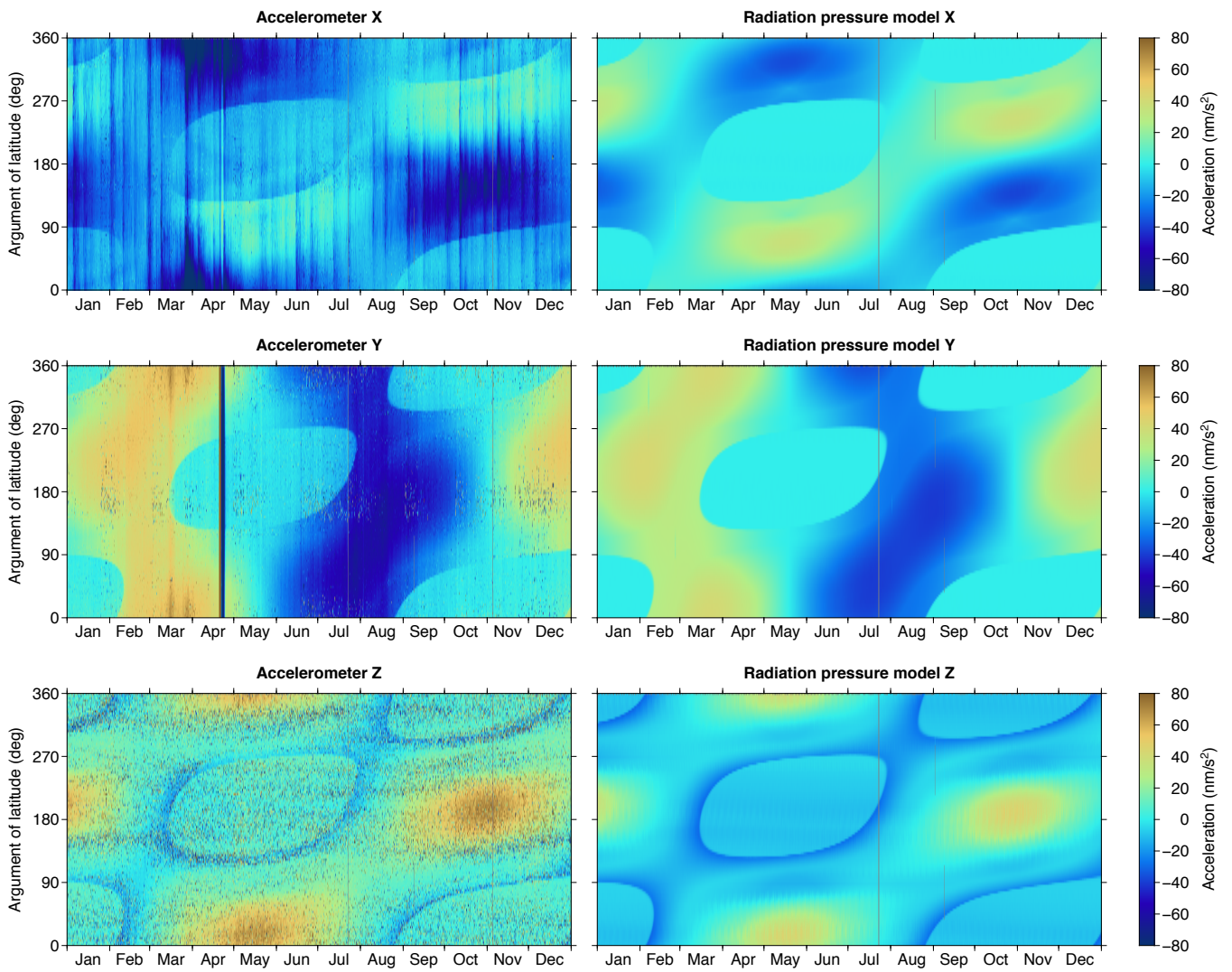
While at low altitudes, and higher levels of solar and geomagnetic activity, the aerodynamic acceleration is the dominant non-gravitational accelerations, in other circumstances, the radiation pressure acceleration is the most influential.

Figure 5 shows a comparison of the measured accelerations on GRACE-A in 2008. GRACE was still at a relatively high altitude at the time, of about 480 km, while solar activity was at its lowest since the beginning of the space age. The accelerations are shown as a function of time on the graph's horizontal axis, and argument of latitude (angle along the orbit from the ascending equator crossing) on the vertical axis, which is useful to show both spatial and temporal variations of the accelerations.

The three rows correspond to the three axes of the satellite body-fixed reference frame, in which the accelerations are measured and modelled. The X-, Y- and Z-axes of the satellite body-fixed frame are kept closely aligned with the along-track, cross-track and nadir directions in the orbit, respectively.

The left row in the figure shows the measured accelerations, while the right row shows the equivalent modelled radiation pressure accelerations. The plots show a good general agreement of the variations along the orbit, and due to the precession of the orbit with respect to the Sun (local time variation). The sharp edges in both plots are due to the eclipses, which happened, for example, over the descending node in May 2008 and . The most significant differences between measurement and model are visible in the X-direction, due to the aerodynamic accelerations, and in the Z-direction, which shows the most noise-like variations, which are actually largely due to the firing of attitude control cold-gas thruster pairs, that are not perfectly balanced, thus causing a residual linear acceleration.

In order to further investigate possible issues in the radiation pressure acceleration modelling, we have made a first-



**Fig. 5.** Calibrated non-gravitational acceleration measurements during 2008 made by the GRACE-A satellite.

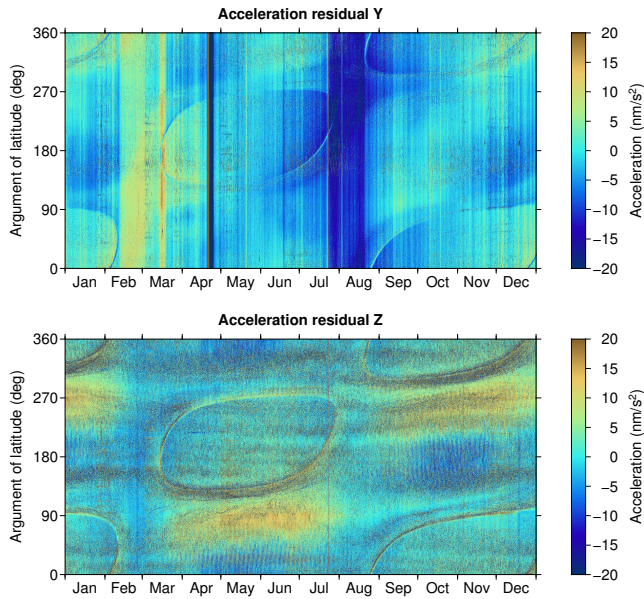


**Fig. 6.** Residuals of the calibrated non-gravitational acceleration measurements made by the GRACE-A satellite, minus the equivalent modelled aerodynamic and radiation pressure accelerations.

order estimate of the densities from the X-axis (along-track) acceleration measurements, and fed this into our aerodynamic model, to arrive at a modelled acceleration in the Y- and Z-axis directions. Both this aerodynamic acceleration model, and the radiation pressure acceleration model shown on the right in Figure 5 have been subtracted from the accelerometer observations to arrive at Figure 6. A comparison of the two Figures, taking into account the differences in the extent of the colour scales, shows that most, but not all, of the accelerations were accurately modelled.

An interesting feature in the residuals is the sharp spike at the eclipse transitions in some months, especially July and

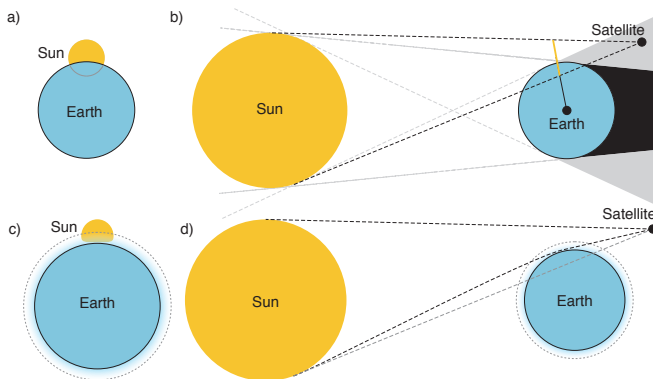


**Fig. 7.** Eclipse geometry, without (top) and with (bottom) the effect of atmospheric absorption and refraction.



**Fig. 8.** The setting Sun photographed from the International Space Station. Images courtesy of the Earth Science and Remote Sensing Unit, NASA Johnson Space Center. Sequence ISS046-E-51636 to ISS046-E-51714.

August. This is believed to be caused by the effects of refraction and absorption of Sunlight in the lower atmosphere, affecting the radiation pressure. These effects, which both bend and attenuate the sunlight around the time of the purely geometric eclipse transition, are particularly difficult to model well. Figure 7 gives an illustration of the geometry of the problem, while Figure 8 shows photos taken from the International Space Station of a sunset over the Pacific. The first photo in the series clearly shows the illumination of the clouds, before any part of the solar disc is visible. Strictly speaking, this causes an Earth albedo radiation pressure acceleration. The solar radiation pressure begins as the first part of the solar disc becomes visible above the horizon in the second photo, taken 20 seconds later. From a purely geometric point of view, the entire solar disc is still behind the Earth at this point. It is only visible because of the refraction by the atmosphere. In subsequent photos, the distortion of the solar disc by the lower atmosphere, and the attenuation by the cloudy atmospheric layer at the bottom, and the clear atmospheric layer above, is readily apparent.

This effect is at the cutting-edge of the current state-of-the-art of non-gravitational force modelling. The effect on the orbit is very small in most cases, and it is mostly important for density and wind determination from the accelerometer measurements.

## 5. CONCLUSIONS

The paper gave several examples of how satellite accelerometer data can be used to evaluate non-gravitational force models, that are traditionally used in orbit propagation and orbit

determination applications. Such models have found a new use in the conversion of accelerometer data into information on thermospheric density and wind speed. The demand for accuracy in these thermospheric data sets by the space science community is currently driving the state-of-the-art in non-gravitational force modelling.

It is likely that these developments could prove beneficial if fed back into precise orbit determination applications. At the same time, the data can be used to demonstrate the applicability of several simplifying assumptions that have been traditionally applied in astrodynamics software.

## References

- [1] E. Doornbos, R. Scharroo, H. Klinkrad, R. Zandbergen, and B. Fritsche, "Improved modelling of surface forces in the orbit determination of ERS and Envisat," *Canadian Journal of Remote Sensing*, vol. 28, no. 4, pp. 535–543, 2002.
- [2] Ch. Reigber, P. Schwintzer, and H. Lühr, "The CHAMP geopotential mission," in *Bollettino di Geofisica Teoretica ed Applicata, Vol. 40, No. 3-4, Sep.-Dec. 1999, Proceedings of the 2nd Joint Meeting of the International Gravity and the International Geoid Commission, Trieste 7-12 Sept. 1998, ISSN 0006-6729*, I. Marson and H. Stükel, Eds., 1999, pp. 285–289.
- [3] B. D. Tapley, S. Bettadpur, M. Watkins, and C. Reigber, "The gravity recovery and climate experiment: Mission overview and early results," *Geophysical Research Letters*, vol. 31, no. 9, pp. n/a–n/a, 2004, L09607.
- [4] M.R. Drinkwater, R. Floberghagen, R. Haagmans, D. Muzi, and A. Popescu, "GOCE: ESA's first Earth Explorer core mission," in *Earth gravity field from space – from sensors to Earth sciences*, G.B. Beutler, M.R. Drinkwater, R. Rummel, and R. von Steiger, Eds., vol. 18 of *Space Sciences Series*, pp. 419–432. Kluwer academic publishers, 2003.
- [5] E. Friis-Christensen, H. Lühr, D. Knudsen, and R. Haagmans, "Swarm - an earth observation mission investigating geospace," *Advances in Space Research*, 2006.
- [6] Eelco Doornbos, *Thermospheric Density and Wind Determination From Satellite Dynamics*, Ph.D. thesis, Delft University of Technology, 2011.
- [7] Eelco Doornbos, Jose van den IJssel, Hermann Lühr, Matthias Förster, and Georg Koppenwallner, "Neutral density and crosswind determination from arbitrarily oriented multiaxis accelerometers on satellites," *Journal of Spacecraft and Rockets*, vol. 47, no. 4, pp. 580–589, 2010.
- [8] L.G. Jacchia, "Revised static models of the thermosphere and exosphere with empirical temperature profiles," *Smithsonian Astrophysical Observatory Special Report*, vol. 332, 1971.
- [9] Bruce R. Bowman, W. Kent Tobiska, Frank A. Marcos, Cheryl Y. Huang, Chin S. Lin, and W.J. Burke, "A new empirical thermospheric density model JB2008 using new solar and geomagnetic indices," *Draft for CIRA 2008*, 2008.
- [10] J.M. Picone, A.E. Hedin, D.P. Drob, and A.C. Aikin, "NRLMSISE-00 empirical model of the atmosphere: Statistical comparisons and scientific issues," *Journal of Geophysical Research*, vol. 107, no. A12, 2002.
- [11] Bruinsma, Sean, "The dtm-2013 thermosphere model," *J. Space Weather Space Clim.*, vol. 5, pp. A1, 2015.
- [12] M.F. Storz, B.R. Bowman, J.I. Branson, S.J. Casali, and W.K. Tobiska, "High accuracy satellite drag model (HASDM)," *Advances in Space Research*, vol. 36, no. 12, pp. 2497–2505, 2005.
- [13] Douglas P. Drob, John T. Emmert, John W. Meriwether, Jonathan J. Makela, Eelco Doornbos, Mark Conde, Gonzalo Hernandez, John Noto, Katherine A. Zawdie, Sarah E. McDonald, Joe D. Huba, and Jeff H. Klenzing, "An update to the horizontal wind model (hwm): The quiet time thermosphere," *Earth and Space Science*, vol. 2, no. 7, pp. 301–319, 2015, 2014EA000089.
- [14] G. Koppenwallner, "Comment on special section: New perspectives on the satellite drag environments of Earth, Mars and Venus," *Journal of Spacecraft and Rockets*, vol. 45, no. 6, pp. 1324–1326, 2008.
- [15] Eric K. Sutton, "Normalized force coefficients for satellites with elongated shapes," *Journal of Spacecraft and Rockets*, vol. 46, no. 1, pp. 112–116, 2009.